Acta Crystallographica Section A
Foundations of Crystallography
ISSN 0108-7673

Received 5 September 2003
Accepted 30 October 2003

Phase-dependent polarization aspects of three-wave X-ray diffraction: an iterative Born approximation

Yuri P. Stetsko,[a,b,c]* Yen-Ru Lee,[b] Mau-Tsu Tang[a] and Shih-Lin Chang[a,b]

[a]National Synchrotron Radiation Research Center, Hsinchu, 300 Taiwan, [b]Department of Physics, National Tsing Hua University, Hsinchu, 300 Taiwan, and [c]Chernovtsy State University, Chernovtsy 58012, Ukraine. Correspondence e-mail: stetsko@nsrrc.org.tw

The iterative Born approximation is derived for three-wave dynamical X-ray diffraction. Dependence of the three-wave diffraction profiles of the diffracted wave on the polarization state of a linearly polarized incident wave is theoretically and experimentally investigated. General conditions of the phase sensitivity as well as the asymmetry of diffraction profiles are obtained from this approximation and compared with direct dynamical calculations. Reasonable qualitative agreement between the results obtained from this iterative approach and the exact dynamical calculation is shown. A new feature of reversing asymmetry of an intensity profile with respect to phase change is theoretically predicted.

1. Introduction

The phase-dependent behavior of multiwave X-ray diffraction has been extensively studied for decades (see, for example, the reviews by Chang, 1984, 1987, 1992, 1998; Colella, 1995; Weckert & Hümmer, 1997). As is well known, the phase information is conveyed in multiwave diffraction processes through the interference between a directly excited Bragg diffracted wave and detoured excited waves, which could be of *Umweganregung* (see Stetsko & Chang, 1999*a*,*b*) or *Aufhellung* types. The resulting angular intensity distribution of a multiply diffracted wave thus depends on the phase sums of the associated structure-factor multiplets involved in the multiwave process and the 180° phase shift of the *Umweg*-excited waves.

On the other hand, much attention has also been paid to the inverse problem – the determination of phases from theoretical (numerical) solutions and measurements. For that purpose, the choice of a phase-sensitive multiwave diffraction is of great practical importance. In fact, in a multiwave diffraction experiment, the phase sensitivity is closely related to the mutual plays between the polarization of the incident and the diffracted waves. Theoretically, the expressions of the diffracted amplitudes and intensities in terms of polarization factors have been derived from the Bethe and Born approximations and Takagi–Taupin treatment (Juretschke, 1982*a*,*b*, 1986; Høier & Marthinsen, 1983; Shen, 1986, 1999, 2000; Hümmer & Billy, 1986; Thorkildsen, 1987; Chang & Tang, 1988; Stetsko, Lin *et al.*, 2001; Shen & Huang, 2001; Thorkildsen *et al.*, 2001; Thorkildsen & Larsen, 2002; and many others). The condition for the occurrence of inversed asymmetry of the diffracted profile with π-polarized incident radiation, compared to a σ-polarized wave, has been obtained (Juretschke, 1986; Shen, 1986). The physics behind this is that for a π-polarized incident wave the projection of the wavefield of the detoured excited wave onto the wavefield of the directly excited wave does not coincide and sometimes is opposite, while for a σ-polarized incident wave these directions always coincide. If the two directions are opposite to each other for the π polarization, an additional phase shift of 180° is introduced into the detoured excited wave, thus causing the inversed asymmetry of the three-wave diffraction profile. The use of unpolarized, linearly polarized or elliptically polarized incident radiation to reveal polarization-dependent phase measurements have also been theoretically and experimentally pursued (Shen & Finkelstein, 1990, 1992; Luh & Chang, 1991; Shen, 1993; Stetsko & Chang, 1999*a*,*b*; Stetsko *et al.*, 1999, 2000; Stetsko, Juretschke *et al.*, 2001; Morelhão & Kycia, 2002; Morelhão, 2003). Despite these important theoretical and experimental results, a general description of the phase-dependent polarization aspects of multiwave X-ray diffraction, especially for arbitrarily selected (intermediate) polarization of the linearly polarized incident radiation, is still lacking. It is therefore the purpose of this paper to give a general formulation, covering both *Umweganregung* and *Aufhellung* processes, and to predict some new polarization phenomena with respect to multiple-wave interaction, which cannot be obtained, in principle, for particular σ and π polarizations. Moreover, the intermediate polarization state of the incident radiation is of practical significance in delineating phase-sensitive multiple-diffraction profiles and in providing accurate determination of the associated phases. In addition, it may be found useful in improving the phase measurement of the recently developed reference-beam stereoscopic imaging

technique (Shen, 1998; Shen *et al.*, 2000; Chang, Chao *et al.*, 1999; Wang *et al.*, 2001; Chao *et al.*, 2002), where a large number of multiple diffractions are involved and the polarization is different for different diffraction cases.

2. Second-order iterative Born approximation

2.1. Superposition of wavefields

The iterative Born approximation for three-wave diffraction proposed by Chang & Tang (1988) and Chang *et al.* (1989) for phase analysis is adopted. Modification is given to include higher-order terms in the approximation so that it could provide qualitative theoretical analysis of the behavior and phase sensitivity of three-wave X-ray diffraction for an arbitrary polarization state of a linearly polarized incident radiation, especially to bring the *Aufhellung* terms into the intensity expression.

Consider a three-wave (O, G, L) X-ray diffraction, in which O, G and L are incident, primary and secondary reflections, respectively. $G - L$ is the coupling reflection between G and L reflections. For the three-wave case, the fundamental equations can be expressed in terms of the electric displacement $\mathbf{D}$ (see, for example, Chang, 1984):

$$\begin{aligned}\mathbf{D}_O &= A_O\chi_{-G}\mathbf{D}_{G[O]} + A_O\chi_{-L}\mathbf{D}_{L[O]}\\ \mathbf{D}_G &= A_G\chi_G\mathbf{D}_{O[G]} + A_G\chi_{G-L}\mathbf{D}_{L[G]}\\ \mathbf{D}_L &= A_L\chi_L\mathbf{D}_{O[L]} + A_L\chi_{L-G}\mathbf{D}_{G[L]},\end{aligned} \tag{1}$$

where the resonance term

$$A_H = 1/(2\varepsilon_H - \chi_O), \tag{2}$$

$2\varepsilon_H = (K_H^2 - k^2)/K_H^2$ ($H \equiv O, G, L$), k is the magnitude of the incident wavevector in vacuum and K_H are the magnitudes of diffracted waves in the crystal. The notation

$$\mathbf{D}_{H_i[H_j]} = -[\mathbf{s}_{H_j} \times (\mathbf{s}_{H_j} \times \mathbf{D}_{H_i})] \tag{3}$$

represents the vector component of $\mathbf{D}_{H_i}$ normal to the unit vector $\mathbf{s}_{H_j} = \mathbf{K}_{H_j}/K_{H_j}$ of the wavevector $\mathbf{K}_{H_j}$. The quantity $\chi_H = -r_e\lambda^2 F_H/(\pi V)$ is the Fourier component of the crystal polarizability and F_H is the structure factor of a reflection H. r_e is the classical radius of the electron, λ is the incident X-ray wavelength and V is the unit-cell volume.

Substituting the third equation of the system (1) into the first two, we obtain

$$\begin{aligned}\mathbf{D}_O = {} & A_O\chi_{-G}\mathbf{D}_{G[O]} + A_O A_L\chi_L\chi_{-L}\mathbf{D}_{O[L][O]}\\ & + A_O A_L\chi_{L-G}\chi_{-L}\mathbf{D}_{G[L][O]}\end{aligned} \tag{4a}$$

$$\begin{aligned}\mathbf{D}_G = {} & A_G\chi_G\mathbf{D}_{O[G]} + A_G A_L\chi_L\chi_{G-L}\mathbf{D}_{O[L][G]}\\ & + A_G A_L\chi_{L-G}\chi_{G-L}\mathbf{D}_{G[L][G]},\end{aligned} \tag{4b}$$

where

$$\mathbf{D}_{H_i[H_j][H_l]} = -[\mathbf{s}_{H_l} \times (\mathbf{s}_{H_l} \times \mathbf{D}_{H_i[H_j]})] \tag{5}$$

is the vector component of $\mathbf{D}_{H_i[H_j]}$ normal to the unit wavevector $\mathbf{s}_{H_l}$.

Equations (4*a*) and (4*b*) are the exact expressions of the recurrent relationship between $\mathbf{D}_G$ and $\mathbf{D}_O$ in the three-wave regime. The three-wave (O, G, L) diffraction can be considered as perturbation to the two-wave (O, G) diffraction that is described by the first terms in the right-hand side of these equations. Equation (4*a*) can be rewritten in an approximate form as

$$\mathbf{D}_O \cong \mathbf{D}_O^{(2)} + A_O A_L\chi_L\chi_{-L}\mathbf{D}_{O[L][O]}^{(2)} + A_O A_L\chi_{L-G}\chi_{-L}\mathbf{D}_{G[L][O]}, \tag{6}$$

where $\mathbf{D}_O^{(2)}$ is the wavefield of the O reflection for the two-wave case. Substituting (6) and the two-wave approximate wavefield, $\mathbf{D}_G^{(2)} = A_G\chi_G\mathbf{D}_{O[G]}^{(2)}$, into the right-hand side of (4*b*), we finally obtain

$$\begin{aligned}\mathbf{D}_G \cong {} & A_G\chi_G\mathbf{D}_{O[G]}^{(2)} + A_G A_L\chi_L\chi_{G-L}\mathbf{D}_{O[L][G]}^{(2)}\\ & - A_G A_O A_L\chi_G\chi_L\chi_{-L}\mathbf{D}_{O[L][O][G]}^{(2)}\\ & - A_G^2 A_L\chi_G\chi_{L-G}\chi_{G-L}\mathbf{D}_{O[G][L][G]}^{(2)}\\ \equiv {} & \mathbf{D}_2 + \mathbf{D}_{Um} + \mathbf{D}_{Au1} + \mathbf{D}_{Au2},\end{aligned} \tag{7}$$

where

$$\mathbf{D}_{H_i[H_j][H_l][H_m]} = -[\mathbf{s}_{H_m} \times (\mathbf{s}_{H_m} \times \mathbf{D}_{H_i[H_j][H_l]})] \tag{8}$$

is the vector component of $\mathbf{D}_{H_i[H_j][H_l]}$ normal to the unit wavevector $\mathbf{s}_{H_m}$. According to Chang & Tang (1988) and Chang *et al.* (1989), (7) is a second-order iterative approximation for $\mathbf{D}_G$. The higher-order terms in (7) are dropped out. The first two terms in (7) are due to the first-order iterative approximation of $\mathbf{D}_G$. In fact, this first-order iterative approximation corresponds to the second-order Born approximation (Shen, 1986). Thus, (7) can be considered as the third-order Born approximation.

The analysis of (7) shows that within the second-order iterative approximation the wavefield $\mathbf{D}_G$ of the primary reflected wave G in the three-wave case can be represented as the superposition of the directly excited wave $\mathbf{D}_2$, the *Umweg*-excited wave $\mathbf{D}_{Um}$ and two *Aufhellung* (see Wagner, 1923) waves, $\mathbf{D}_{Au1}$ and $\mathbf{D}_{Au2}$. The meaning of these two terms will be clear in the latter consideration in §3. It should be noted that in contrast to the present representation the second-order iterative approximation shown by Chang & Tang (1988) was not complete and contained only one *Aufhellung* term $\mathbf{D}_{Au2}$.

Equation (7) can be rewritten as

$$\begin{aligned}\mathbf{D}_G \cong {} & A_G\chi_G[\mathbf{D}_{O[G]}^{(2)} + A_L|\chi_L||\chi_{G-L}||\chi_G|^{-1}\exp(i\delta)\mathbf{D}_{O[L][G]}^{(2)}\\ & - A_O A_L|\chi_L||\chi_{-L}|\mathbf{D}_{O[L][O][G]}^{(2)}\\ & - A_G A_L|\chi_{L-G}||\chi_{G-L}|\mathbf{D}_{O[G][L][G]}^{(2)}],\end{aligned} \tag{9}$$

where

$$\delta = -\delta_G + \delta_L + \delta_{G-L} \tag{10}$$

is the triplet phase invariant and δ_H ($H \equiv G, L, G - L$) is the phase of the structure factor of the H reflection. For simplicity, in (9), instead of the product $\chi_H\chi_{-H}$, we consider $|\chi_H||\chi_{-H}|$, which is correct for cases with photon energies far from the absorption edges of the involved atoms where the phase sum $\delta_H + \delta_{-H}$ is close to zero. At the absorption edges, where Friedel's law is no longer valid, the values of the phase sum

can differ from zero dramatically and should be taken into account in theoretical considerations (see Stetsko, Lin *et al.*, 2001).

2.2. Polarization factors of wavefields

Consider a linearly polarized incident wave with the wavefield $\mathbf{D}_O = D_O\mathbf{p}_O$, where the arbitrary unit polarization vector $\mathbf{p}_O = \alpha\boldsymbol{\sigma} + \beta\boldsymbol{\pi}_O$ with $\alpha = \cos\omega$ and $\beta = \sin\omega$, ω being the angle between $\mathbf{p}_O$ and the $\boldsymbol{\sigma}$ vector (see Fig. 1). The polarization unit vectors are defined conventionally as $\boldsymbol{\sigma} \equiv \boldsymbol{\sigma}_O \equiv \boldsymbol{\sigma}_G = [\mathbf{s}_G \times \mathbf{s}_O]/|[\mathbf{s}_G \times \mathbf{s}_O]|$, $\boldsymbol{\pi}_O = [\mathbf{s}_O \times \boldsymbol{\sigma}]$, $\boldsymbol{\pi}_G = [\mathbf{s}_G \times \boldsymbol{\sigma}]$. Within the framework of the kinematical approximation (see also Zachariasen, 1965; Caticha-Ellis, 1969; Shen & Finkelstein, 1992; Stetsko & Chang, 1999*b*), the vector component $\mathbf{D}^{(2)}_{O[G]}$ of the wavefield $\mathbf{D}_G$ of (7) can be given by

$$\mathbf{D}^{(2)}_{O[G]} = (\alpha\boldsymbol{\sigma}_{O[G]} + \beta\boldsymbol{\pi}_{O[G]})D_O \equiv \mathbf{p}_2 D_O, \tag{11}$$

where from (3) $\boldsymbol{\sigma}_{O[G]} = \boldsymbol{\sigma}$ and $\boldsymbol{\pi}_{O[G]} = \boldsymbol{\pi}_O - (\mathbf{s}_G \cdot \boldsymbol{\pi}_O)\mathbf{s}_G$, and $\mathbf{p}_2$ is the polarization vector of the directly diffracted wave. Similar to $\mathbf{D}^{(2)}_{O[G]}$, the vector components $\mathbf{D}^{(2)}_{O[L][G]}$, $\mathbf{D}^{(2)}_{O[L][O][G]}$ and $\mathbf{D}^{(2)}_{O[G][L][G]}$ of the wavefield $\mathbf{D}_G$ can be given by

$$\mathbf{D}^{(2)}_{O[L][G]} = (\alpha\boldsymbol{\sigma}_{O[L][G]} + \beta\boldsymbol{\pi}_{O[L][G]})D_O \equiv \mathbf{p}_{Um} D_O, \tag{12a}$$

$$\mathbf{D}^{(2)}_{O[L][O][G]} = (\alpha\boldsymbol{\sigma}_{O[L][O][G]} + \beta\boldsymbol{\pi}_{O[L][O][G]})D_O \equiv \mathbf{p}_{Au1} D_O, \tag{12b}$$

$$\mathbf{D}^{(2)}_{O[G][L][G]} = (\alpha\boldsymbol{\sigma}_{O[G][L][G]} + \beta\boldsymbol{\pi}_{O[G][L][G]})D_O \equiv \mathbf{p}_{Au2} D_O, \tag{12c}$$

with the respective polarization vectors $\mathbf{p}_{Um}$, $\mathbf{p}_{Au1}$ and $\mathbf{p}_{Au2}$. All the components $\mathbf{D}^{(2)}_{O[G]}$, $\mathbf{D}^{(2)}_{O[L][G]}$, $\mathbf{D}^{(2)}_{O[L][O][G]}$ and $\mathbf{D}^{(2)}_{O[G][L][G]}$ of the wavefield $\mathbf{D}_G$ as well as the corresponding polarization vectors $\mathbf{p}_2$, $\mathbf{p}_{Um}$, $\mathbf{p}_{Au1}$ and $\mathbf{p}_{Au2}$ are normal to the wavevector $\mathbf{s}_G$ (see Fig. 1) and, therefore, can be represented in the coordinate system $(\boldsymbol{\sigma}, \boldsymbol{\pi}_G)$. The scalar products of the vectors of (11) and (12) with the unit vectors $\boldsymbol{\sigma}$ and $\boldsymbol{\pi}_G$ give the polarization factors of the diffracted wavefields. According to (3), (5) and (8), the components of the polarization vector $\mathbf{p}_2$ are given by $P^{\sigma}_2(\sigma) = (\boldsymbol{\sigma}_{O[G]} \cdot \boldsymbol{\sigma}) = 1$, $P^{\pi}_2(\sigma) = (\boldsymbol{\sigma}_{O[G]} \cdot \boldsymbol{\pi}_G) = 0$, $P^{\sigma}_2(\pi) = (\boldsymbol{\pi}_{O[G]} \cdot \boldsymbol{\sigma}) = 0$, $P^{\pi}_2(\pi) = (\boldsymbol{\pi}_{O[G]} \cdot \boldsymbol{\pi}_G) = (\boldsymbol{\pi}_O \cdot \boldsymbol{\pi}_G) = \cos 2\theta_G$, which are the well known polarization factors for the directly (primary) diffracted wave $\mathbf{D}^{(2)}_{O[G]}$. The terms

$$P^{\sigma}_{Um}(\sigma) = (\boldsymbol{\sigma}_{O[L][G]} \cdot \boldsymbol{\sigma}) = P^{\sigma}_2(\sigma) - (\mathbf{s}_L \cdot \boldsymbol{\sigma})^2, \tag{13a}$$

$$P^{\pi}_{Um}(\sigma) = (\boldsymbol{\sigma}_{O[L][G]} \cdot \boldsymbol{\pi}_G) = P^{\pi}_2(\sigma) - (\mathbf{s}_L \cdot \boldsymbol{\sigma})(\mathbf{s}_L \cdot \boldsymbol{\pi}_G), \tag{13b}$$

$$P^{\sigma}_{Um}(\pi) = (\boldsymbol{\pi}_{O[L][G]} \cdot \boldsymbol{\sigma}) = P^{\sigma}_2(\pi) - (\mathbf{s}_L \cdot \boldsymbol{\pi}_O)(\mathbf{s}_L \cdot \boldsymbol{\sigma}), \tag{13c}$$

$$P^{\pi}_{Um}(\pi) = (\boldsymbol{\pi}_{O[L][G]} \cdot \boldsymbol{\pi}_G) = P^{\pi}_2(\pi) - (\mathbf{s}_L \cdot \boldsymbol{\pi}_O)(\mathbf{s}_L \cdot \boldsymbol{\pi}_G) \tag{13d}$$

are the components of the polarization vector $\mathbf{p}_{Um}$ for the *Umweg*-exited wave $\mathbf{D}^{(2)}_{O[L][G]}$ (see also Shen & Finkelstein, 1992; Stetsko & Chang, 1999*b*) and

$$P^{\sigma}_{Au1}(\sigma) = (\boldsymbol{\sigma}_{O[L][O][G]} \cdot \boldsymbol{\sigma}) = P^{\sigma}_{Um}(\sigma), \tag{14a}$$

$$P^{\pi}_{Au1}(\sigma) = (\boldsymbol{\sigma}_{O[L][O][G]} \cdot \boldsymbol{\pi}_G) = P^{\pi}_{Um}(\sigma) + (\mathbf{s}_L \cdot \boldsymbol{\sigma})(\mathbf{s}_O \cdot \boldsymbol{\pi}_G)(\mathbf{s}_L \cdot \mathbf{s}_O), \tag{14b}$$

$$P^{\sigma}_{Au1}(\pi) = (\boldsymbol{\pi}_{O[L][O][G]} \cdot \boldsymbol{\sigma}) = P^{\sigma}_{Um}(\pi), \tag{14c}$$

$$P^{\pi}_{Au1}(\pi) = (\boldsymbol{\pi}_{O[L][O][G]} \cdot \boldsymbol{\pi}_G) = P^{\pi}_{Um}(\pi) + (\mathbf{s}_L \cdot \boldsymbol{\pi}_O)(\mathbf{s}_O \cdot \boldsymbol{\pi}_G)(\mathbf{s}_L \cdot \mathbf{s}_O) \tag{14d}$$

and

$$P^{\sigma}_{Au2}(\sigma) = (\boldsymbol{\sigma}_{O[G][L][G]} \cdot \boldsymbol{\sigma}) = P^{\sigma}_{Um}(\sigma), \tag{15a}$$

$$P^{\pi}_{Au2}(\sigma) = (\boldsymbol{\sigma}_{O[G][L][G]} \cdot \boldsymbol{\pi}_G) = P^{\pi}_{Um}(\sigma), \tag{15b}$$

$$P^{\sigma}_{Au2}(\pi) = (\boldsymbol{\pi}_{O[G][L][G]} \cdot \boldsymbol{\sigma}) = P^{\sigma}_{Um}(\pi) + (\mathbf{s}_G \cdot \boldsymbol{\pi}_O)(\mathbf{s}_L \cdot \boldsymbol{\sigma})(\mathbf{s}_L \cdot \mathbf{s}_G), \tag{15c}$$

$$P^{\pi}_{Au2}(\pi) = (\boldsymbol{\pi}_{O[G][L][G]} \cdot \boldsymbol{\pi}_G) = P^{\pi}_{Um}(\pi) + (\mathbf{s}_G \cdot \boldsymbol{\pi}_O)(\mathbf{s}_L \cdot \boldsymbol{\pi}_G)(\mathbf{s}_L \cdot \mathbf{s}_G) \tag{15d}$$

are the components of the polarization vectors $\mathbf{p}_{Au1}$ and $\mathbf{p}_{Au2}$ for *Aufhellung*-exited waves $\mathbf{D}^{(2)}_{O[L][O][G]}$ and $\mathbf{D}^{(2)}_{O[G][L][G]}$, respectively. The symbols σ and π in the brackets on the left-hand side of (13)– (15) indicate the polarization state of the incident wave. The polarization vectors $\mathbf{p}_2$, $\mathbf{p}_{Um}$, $\mathbf{p}_{Au1}$ and $\mathbf{p}_{Au2}$ depend on the wavelength and the polarization state, specified by the angle ω, of the incident wave. They generally are not collinear (see Fig. 1). For small values of the Bragg angles θ_G, θ_L and θ_{G-L} of the primary, secondary and coupling reflections, the angles between the polarization vectors are also small (around several degrees), while when at least one Bragg angle is close to 45° the angles between the polarization vectors can be arbitrarily large.

2.3. Intensity

Approximation is employed to give explicit expressions for the diffracted intensities. The approximation is of kinematical nature, and is therefore rather rough. However, it allows an equation for the intensities to be obtained in a simple form, which is convenient for analysis. Moreover, the analytical expression gives a better physics insight into the multiple-wave interaction, which is not attainable from direct and exact dynamical calculations. In the present paper, we are interested in correlating, on a qualitative basis, the proposed approximation with the direct dynamical calculations for the diffracted intensity profiles. Comparison of the results obtained from the two approaches is also given.

The resonance terms A_O and A_G are considered, under the proposed approximation, as the two-wave dynamical solution. For simplicity, we consider here the symmetrical Bragg primary reflection G for a semi-infinite crystal. According to Pinsker (1977), the condition $A_O = A_G$ can be used for the modes of propagation that make a major contribution to the

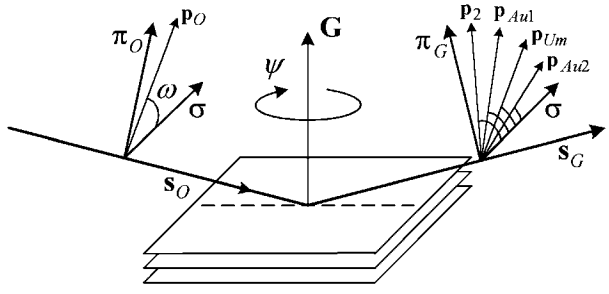

Figure 1
Representation of the polarization vectors for primary G reflection of the three-wave diffraction.

intensities of the transmitted and the diffracted waves. Hereafter, A_O in (9) is replaced by A_G.

Under the proposed approximation, the resonance term A_L is given by (see Chang, 1998)

$$A_L = 1/(\psi - i\eta_\psi/2), \tag{16}$$

where $\eta_\psi = |L_F||\chi_O|\gamma_L/\gamma_O$ (see Chang *et al.*, 1989) is the fundamental width of the three-wave diffraction in ψ scans and $L_F = 1/(\boldsymbol{\sigma}\cdot\mathbf{s}_L)\cos\theta_G$ is a Lorentz factor. The $-$ sign in (16) corresponds to the situation when the positive direction of the azimuthal rotation ψ is accompanied by the movement of the reciprocal-lattice point of the secondary reflection L towards the interior of the Ewald sphere. Equation (16) describes the contribution of the azimuth ψ angular distribution of the diffracted wave in the vicinity of the exact three-wave position $\psi = 0$. The change of the azimuthal angle ψ by crossing this three-wave position is accompanied with a phase change of 180° in the resonance term A_L. According to (9), this corresponds to the same change of phase of the *Umweg*-excited wave (see also Hümmer & Billy, 1986; Shen & Finkelstein, 1992; Stetsko & Chang, 1999*b*) and the *Aufhellung*-excited waves. The complex square of the A_L is Lorentzian.

In addition to the intensity distributions *versus* the azimuthal angle ψ represented in the existing version of the iterative approximation (Chang & Tang, 1988; Chang *et al.*, 1989), we also consider the three-wave intensity distribution along the Bragg direction $\theta = \Delta\theta_G$. As is well known, in the case of the symmetrical Bragg diffraction and σ-polarized incident radiation, the resonance term A_G along the θ direction is represented by

$$A_G = 1/(\theta\sin 2\theta_G + i\,\mathrm{Im}\chi_O + g), \tag{17}$$

where $g = \pm[(\theta\sin 2\theta_G + i\,\mathrm{Im}\,\chi_O)^2 - \chi_G\chi_{-G}]^{1/2}$ with $\mathrm{Im}\,g < 0$. For a nonabsorbing crystal, the fundamental width η_θ of the total reflection region is $\eta_\theta = 2|\chi_G|/\sin 2\theta_G$. It is not easy to obtain from (17) an analytical expression for the intensity of the diffracted wave G in the three-wave case. Therefore, we make here a rather rough approximation for the resonance term A_G similar to (16) as

$$A_G = 1/[\sin 2\theta_G(\theta - i\eta_\theta/2)]. \tag{18}$$

However, (18) has the following merits. It behaves in a way similar to (17), *i.e.* the phase change of 180° in the vicinity of the exact Bragg position $\theta = 0$, and has the same width η_θ. Equation (18) can easily be used to derive an analytical expression for the intensity of the diffracted wave G in the three-wave case. The $-$ sign in (18) corresponds to the situation when the positive direction of the Bragg rotation θ is accompanied by the movement of the reciprocal-lattice point of the primary reflection G towards the interior of the Ewald sphere.

The intensity of the diffracted wave is convenient to be represented in the universal dimensionless angle parameters $\psi_u = 2\psi/\eta_\psi$ and $\theta_u = 2\theta/\eta_\theta$, the reduced angle parameters. Taking into account (9), (16) and (18), the three-wave intensity is given by

$$\begin{aligned} I_G(\psi_u,\theta_u) &= \mathbf{D}_G\mathbf{D}_G^* \\ &= d_2^2/(\theta_u^2+1) + [2d_{2Um}(\psi_u\cos\delta - \sin\delta) + d_{Um}^2] \\ &\quad\times[(\psi_u^2+1)(\theta_u^2+1)]^{-1} + [2d_{2Au}(\psi_u\theta_u - 1) \\ &\quad + 2d_{UmAu}(\theta_u\cos\delta + \sin\delta) + d_{Au}^2]/(\psi_u^2+1)(\theta_u^2+1)^2, \end{aligned} \tag{19}$$

where the scalar products

$$\begin{aligned} d_2^2 &= p_2^2 D_O^2, \\ d_{2Um} &= f(\mathbf{p}_2\cdot\mathbf{p}_{Um})D_O^2, \\ d_{2Au} &= f_L(\mathbf{p}_2\cdot\mathbf{p}_{Au1})D_O^2 + f_{G-L}(\mathbf{p}_2\cdot\mathbf{p}_{Au2})D_O^2, \\ d_{Um}^2 &= f^2 p_{Um}^2 D_O^2, \\ d_{UmAu} &= ff_L(\mathbf{p}_{Um}\cdot\mathbf{p}_{Au1})D_O^2 + ff_{G-L}(\mathbf{p}_{Um}\cdot\mathbf{p}_{Au2})D_O^2, \\ d_{Au}^2 &= |f_L\mathbf{p}_{Au1} + f_{G-L}\mathbf{p}_{Au2}|^2 D_O^2 \end{aligned}$$

and

$$\begin{aligned} f &= w_L|\chi_L||\chi_{G-L}|/|\chi_G||\chi_O| \equiv w_L|F_L||F_{G-L}|/|F_G||F_O|, \\ f_L &= w_L|\chi_L||\chi_{-L}|/|\chi_G||\chi_O| \equiv w_L|F_L||F_{-L}|/|F_G||F_O|, \\ f_{G-L} &= w_L|\chi_{L-G}||\chi_{G-L}|/|\chi_G||\chi_O| \equiv w_L|F_{L-G}||F_{G-L}|/|F_G||F_O|, \end{aligned}$$

and the factor $w_L = 2\gamma_O/|L_F\gamma_L|$.

A highly collimated incident beam in the azimuthal direction is usually required in multiwave diffraction experiments to obtain well resolved peak profiles, while the condition of collimation in the Bragg direction can be somewhat relaxed. Therefore, to compare with experimental results, the semi-integral $I_G(\psi_u) = \int_{-\infty}^{\infty} I_G(\psi_u,\theta_u)\,\mathrm{d}\theta_u$ for intensity will be considered later on. According to (19),

$$\begin{aligned} I_G(\psi_u) &= I_2 + I_D(\psi_u,\delta) + I_I(\psi_u) \\ &= \pi d_2^2 + \pi(A\psi_u\cos\delta - B\sin\delta)/(\psi_u^2+1) + \pi C/(\psi_u^2+1) \\ &= \pi d_2^2[1 + (A_n\psi_u\cos\delta - B_n\sin\delta + C_n)/(\psi_u^2+1)], \end{aligned} \tag{20}$$

where the parameters $A = 2d_{2Um}$, $B = 2d_{2Um} - d_{UmAu}$, $C = d_{Um}^2 + d_{Au}^2/2 - d_{2Au}$, and $A_n = A/d_2^2$, $B_n = B/d_2^2$ and $C_n = C/d_2^2$ are the normalized parameters. I_2 is the two-wave intensity, $I_D(\psi_u,\delta)$ is the phase-dependent part and $I_I(\psi_u)$ is the phase-independent part of the three-wave intensity. The analysis of the parameters of (20) allows one to obtain the well known behavior of a three-wave diffraction as well as to predict new behavior unreported in the literature.

It should also be noted that the existing theoretical approximations, for example the distorted-wave Born approximation (Shen, 1999, 2000; Shen & Huang, 2001), Takagi–Taupin treatment (Thorkildsen *et al.*, 2001; Thorkildsen & Larsen, 2002) or Bethe approximation (Stetsko, Lin *et al.*, 2001), give for different cases of Bragg and Laue three-wave diffraction a much better agreement with numerical solutions than that represented in the present paper. However, in most cases, the obtained analytical expressions complicate the analysis of phase-dependent polarization aspects of three-wave diffraction and hinder the possibility of predicting new phase behavior on a qualitative basis. It is, therefore, the purpose of the present paper to provide such possibilities.

3. Main behavior of three-wave diffraction

By the main behavior of a three-wave diffraction, we mean the separation of the contributions of the different components of the wavefield (9) to the resultant intensity when one of the Fourier components of the crystal polarizability (or the structure factors) of the involved reflections is hypothetically considered as negligibly small. These contributions are investigated as an example for the Si(000, 331, 404) three-wave diffraction with σ-polarized incident radiation of 1 Å wavelength. Here and later on, the primary reflection 331 is a symmetrical Bragg reflection. The intensity profiles I_G obtained from the exact dynamical calculation (see Stetsko & Chang, 1997) for $\delta = 0^\circ$ are shown in Fig. 2. The calculated profiles based on the present approximation are given in the inset for qualitative comparison. The profiles of the solid curve are the calculation for the actual three-wave case, where three strong reflections are involved, *i.e.* $|\chi_G|, |\chi_L|, |\chi_{G-L}| \gg 0$. The values of the normalized parameters of (20) are in a typical relation for the diffraction with all strong reflections: $|C_n| < B_n < A_n$ and $C_n < 0$ ($A_n = 0.62$, $B_n = 0.43$ and $C_n = -0.31$). The diffracted intensity I_G *versus* ψ, first decreasing then increasing, exhibits the characteristic asymmetry for $\delta = 0^\circ$. The curves with dashed line, open circles and solid circles are the calculated profiles with $\chi_G = 0$, $\chi_L = 0$ and $\chi_{G-L} = 0$, respectively. The intensity asymmetry related to phase is hardly seen in these three hypothetical situations because the three-wave interaction is null owing to $\chi_{-G}\chi_L\chi_{G-L} = 0$. The calculated curves in the inset are in good qualitative agreement with those of the exact calculation. Note that $\theta_G = 23.7^\circ$ in this case.

As is well known, the *Umweg*-excited wave can be obtained when the Fourier component of the crystal polarizability of the primary reflection G is negligibly small, $|\chi_G| \to 0$. In this case, only the second wavefield $\mathbf{D}_{Um}$ of (7) is significant ($\mathbf{D}_G \cong \mathbf{D}_{Um}$). All parameters of (20) are negligibly smaller than d_{Um}^2 of C, *i.e.* the values of I_2 and $I_D(\psi_u, \delta)$ are negligibly smaller than $I_I(\psi_u)$. The dashed curves for this hypothetical case $|\chi_G| = 0$ with the parameter $C > 0$ is the intensity distribution $I_G(\psi_u) = I_I(\psi_u)$, which is a Lorenzian. For the representation of all curves of the inset of Fig. 2 on the same scale, the intensity $I_G(\psi_u)$ for the case $|\chi_G| = 0$ is normalized by the two-wave intensity $I_{2(\text{actual})}$ for the actual case ($|\chi_G| \gg 0$). On this scale, the modified parameter $C/d_{2(\text{actual})}^2 = 0.29$.

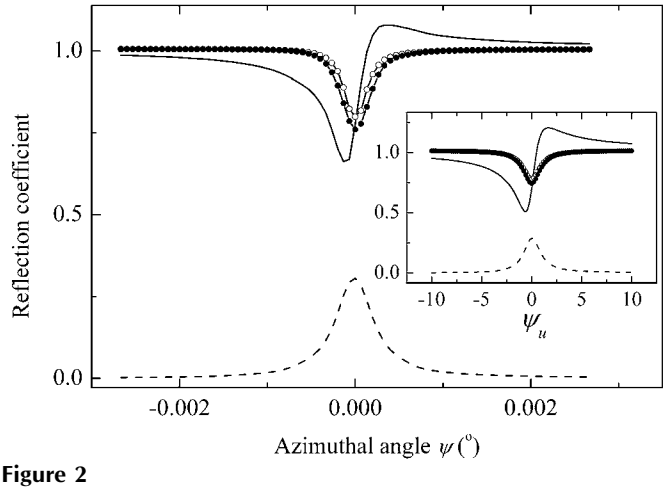

Figure 2
Calculated profiles for Si(000, 331, 404) three-wave diffraction for the σ-polarized incident radiation with $\lambda = 1$ Å. The solid curve corresponds to the actual case, and curves with dashed line, open circles and solid circles correspond to $\chi_G = 0$, $\chi_L = 0$ and $\chi_{G-L} = 0$, respectively. Intensities are normalized with the two-wave intensity for the actual case. Inset: profiles calculated according to the iterative approximation with the same conditions.

When the Fourier component of the crystal polarizability of the coupling reflection $G - L$ is negligibly small, $|\chi_{G-L}| \to 0$, the electric wavefield of the diffracted wave can be represented by $\mathbf{D}_G \cong \mathbf{D}_2 + \mathbf{D}_{Au1}$. The values of the parameters A_n and B_n of (20) are negligibly small. The intensity is then $I_G(\psi_u) = I_2 + I_I(\psi_u)$ with $C_n = (d_{Au}^2/2 - d_{2Au})/d_2^2$. The curves with solid circles are calculated for $|\chi_{G-L}| = 0$. The parameter C_n is negative ($C_n = -0.27$) and, therefore, the intensity $I_G(\psi_u)$ can be considered as a constant intensity background minus a Lorentzian, *i.e.* the intensity is of the *Aufhellung* type. In §2.1, the wavefield $\mathbf{D}_{Au1}$ is referred to as the wavefield of the *Aufhellung* type.

The same situation takes place when the Fourier component of the crystal polarizability of the secondary reflection L is negligibly small, $|\chi_L| \to 0$. The electric wavefield of the diffracted wave can be represented by $\mathbf{D}_G \cong \mathbf{D}_2 + \mathbf{D}_{Au2}$ and the intensity $I_G(\psi_u) = I_2 + I_I(\psi_u)$ with $C_n = (d_{Au}^2/2 - d_{2Au})/d_2^2$. The curves with open circles show the characteristic *Aufhellung* feature. For this hypothetical case, $C_n = -0.24$.

4. Inversed asymmetry of peak profiles

In the introduction of the present paper, we gave a brief explanation of the sense of the inversion of the peak-profile asymmetry for the π-polarized incident radiation compared to the σ-polarized radiation. For the σ-polarized incident radiation, the parameter A_n of (20) is always positive, while for the π-polarized radiation the parameter A_n can be negative and the inversed peak-profile asymmetry occurs (see also Weckert & Hümmer, 1997; Larsen & Thorkildsen, 1998; Stetsko & Chang, 1999*b*). However, situations can occur when the peak profiles for the σ- and π-polarized radiation are of the same asymmetry while for the intermediate ($\omega \neq 0$ or $\pm 90^\circ$) polarization state of the incident radiation the peak asymmetry is inversed. This situation can be realized in a rather wide spectral region when the Bragg angles of the primary, the secondary or/and the coupling reflections are rather close to 45°. The general condition of the inversed peak asymmetry for the intermediate (ω) polarization compared to the σ polarization is given by

$$r(\omega) \equiv (\mathbf{p}_2 \cdot \mathbf{p}_{Um}) < 0, \tag{21}$$

when the angle between the polarization vectors $\mathbf{p}_2$ and $\mathbf{p}_{Um}$ of the primary and *Umweg*-exited waves is obtuse or, which is the same, when the parameter A_n is negative.

Fig. 3 shows the calculated profiles of the Si(000, 331, 404) three-wave diffraction and $\lambda = 1.52$ Å for various linear polarization conditions. In this case, $\theta_G = \theta_{G-L} = 37.6^\circ$ and $\theta_G =$

52.3°. In Fig. 3, the σ- ($\omega = 0°$) and π-polarized ($\omega = \pm 90°$) diffraction profiles exhibit the same proper asymmetry for $\delta = 0°$, *i.e.* first decreasing then increasing. The same peak-profile asymmetry takes place for the incident polarization $-90 < \omega < 0°$, where the parameter $r(\omega)$ of (21) is positive, while the inversed asymmetry is observed for the incident polarization $30 \leq \omega \leq 70°$, where the parameter $r(\omega)$ is negative. Moreover, for the intermediate polarization state of the incident wave, the asymmetry of the peak profiles is much more clearly seen owing to partial suppression of the primary intensity and the comparably large intensity change near the three-wave position that will be considered in §5.

The experimental verification of the theoretical results was carried out at the 1–9 keV bending-magnet beamline BL15B of the National Synchrotron Radiation Research Center with the use of the UHV-compatible six-circle X-ray diffractometer (Gau *et al.*, 2001) with κ geometry. For the detailed experimental conditions, see Stetsko *et al.* (2000). Fig. 4 shows good agreement of the experimental results with the theoretical (calculated) ones (Fig. 3). The comparable broadening and lower visibility of the experimental profiles are due to the convolution with the instrumental functions of the incident beam. These experimental and theoretical results were represented for the first time at the XVIII IUCr Congress and General Assembly (Stetsko *et al.*, 1999).

5. Phase behavior and phase sensitivity

In the present section, we consider fundamentally different cases with different phase behavior and phase sensitivity of three-wave diffraction. Several factors affecting the phase behavior and phase sensitivity are described. Different combinations of values of the normalized parameters A_n, B_n and C_n give different results. These factors are: the numbers of strong and weak reflections involved for the primary, secondary and coupling reflections, the values of Bragg angles of these reflections and the polarization state of the incident radiation.

All figures, Figs. 5–12, of §5 show the calculated profiles for the hypothetical values of the triplet phase $\delta = -90°$ (open circles), $\delta = 0°$ (solid line), $\delta = 90°$ (solid circles) and $\delta = 180°$ (dashed line). Again, the calculations with the proposed approximation are shown in the insets.

5.1. Bragg angles far from 45°

Here we consider different cases of three-wave diffraction for the GaAs single crystal with different combinations of strong and weak reflections among the primary, secondary and coupling reflections, and with rather small Bragg angles of all the reflections.

According to the first-order iterative approximation, the parameter B_n is exactly equal to A_n. From the second-order iterative approximation proposed here, the value of the parameter B_n is rather close to A_n for the cases when Bragg angles of all the reflections are much less than 45° (see Chang *et al.*, 2002, for macromolecular crystals). With increasing values of Bragg angles, the difference between the values of parameters B_n and A_n is also increased. However, when the Bragg angles are still less than 45°, so that the polarization factors of the primary, *Umweg*- and *Aufhellung*-excited waves [equations (13)–(15)] have no strong influence upon the change of the values of parameters A_n and B_n with the change of the polarization state (ω) of the incident radiation, the values of parameters A_n and B_n are both positive. In these cases, three-wave diffraction exhibits the well known 'usual' (the same as for the σ-polarized incident radiation) phase-dependent order of peak-profile asymmetry that is independent of ω. The 'usual' order means that the peak profiles I_G *versus* ψ are: asymmetric for $\delta = 0°$ and $\delta = 180°$, so that the intensity first decreases then increases for $\delta = 0°$ and first increases then decreases for $\delta = 180°$; and the profiles are practically symmetric for $\delta = -90°$ and $\delta = 90°$, so that the

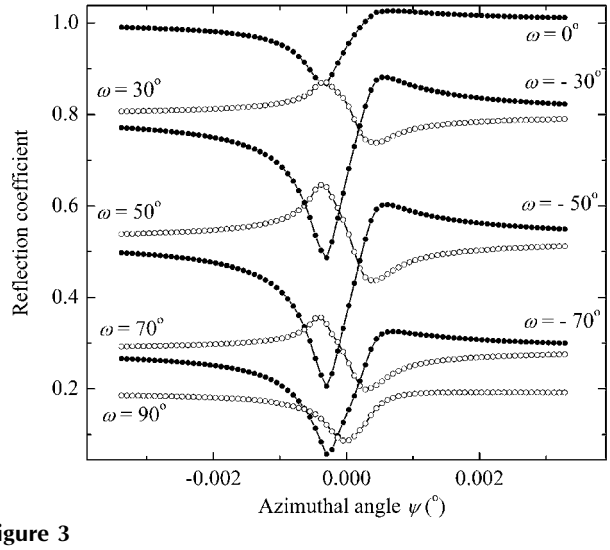

Figure 3
Calculated profiles for Si(000, 331, 404) three-wave diffraction for different polarizations ω of the incident radiation indicated in the figure, λ = 1.52 Å. Intensities are normalized with the two-wave intensity for $\omega = 0°$.

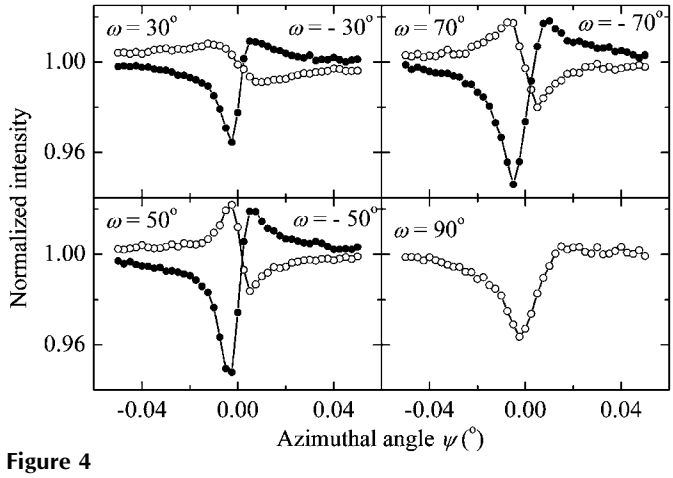

Figure 4
Intensity profiles for Si(000, 331, 404) three-wave diffraction for different polarizations ω of the incident radiation indicated in the figure, λ= 1.52 Å. For convenience of presentation, the intensities are normalized with the individual two-wave intensities.

intensity for $\delta = -90^\circ$ is stronger than for $\delta = 90^\circ$. The phase behavior and phase sensitivity of three-wave diffraction for such small Bragg angles are not strongly dependent on the polarization state of the incident radiation. These cases with different combinations of strong and weak reflections are considered in this section.

5.1.1. All strong reflections. In Fig. 5, the GaAs(000, 111, 220) three-wave diffraction for $\lambda = 1.24$ Å and π-polarized incident radiation ($\omega = 90^\circ$) is subjected to the dynamical calculation. The Bragg angles of the reflections are $\theta_G = \theta_{G-L} = 10.9^\circ$ and $\theta_L = 18.1^\circ$. The conditions among the parameters A_n, B_n and C_n are $|C_n| < B_n < A_n$ and $C_n < 0$, $A_n = 0.60$, $B_n = 0.47$ and $C_n = -0.28$. The asymmetries of peak profiles are very consistent with the rather high phase-sensitive behavior for three-wave diffraction. This means that the peak profiles for $\delta = 0^\circ$ and $\delta = 180^\circ$ are strongly asymmetric. And the peak profile for $\delta = 90^\circ$ is of *Aufhellung* type, while for $\delta = -90^\circ$ it is of *Umweg* type. Owing to the negative value of the parameter C_n (and still $|C_n| < B_n$), the *Aufhellung* component of (7) slightly dominates in this diffraction, which is typical for diffraction with all strong reflections.

5.1.2. Weak primary and strong secondary and coupling reflections. Fig. 6 shows the calculation results for GaAs(000, 222, 311) diffraction with $\lambda = 1.24$ Å and σ-polarized incident radiation, where the primary reflection 222 is weak. The Bragg angles of reflections are $\theta_G = 22.3$, $\theta_L = 21.3$ and $\theta_{G-L} = 10.9^\circ$. The values of parameters A_n and B_n are much smaller than the positive C_n, *i.e.* $A_n = 5.0$, $B_n = 3.7$ and $C_n = 15.9$. Because $C \gg 1$, the intensity profiles show *Umweg*-type features (peaks), *i.e.* the *Umweg* component of (7) strongly dominates in the diffraction. The phase sensitivity of the profiles is low, which is typical for such diffraction. The weak asymmetry of peak profiles is observed for $\delta = 0^\circ$ and $\delta = 180^\circ$, while there is no qualitative difference between $\delta = -90^\circ$ and $\delta = 90^\circ$ cases.

5.1.3. Weak secondary and strong primary and coupling reflections. Fig. 7 shows the calculated results for GaAs(000, 311, 222) diffraction with $\lambda = 1.24$ Å and π-polarized incident radiation where the secondary reflection is weak. The values $|A_n|$ and $|B_n|$ are much smaller than $|C_n|$, where C_n is negative ($A_n = 0.12$, $B_n = 0.07$ and $C_n = -0.45$). Therefore, the *Aufhellung* component of (7) strongly dominates in the diffraction. Similar to the above-mentioned case, the phase sensitivity of the profiles is low. Again, the weak asymmetry of peak profiles is observed for $\delta = 0^\circ$ and $\delta = 180^\circ$, while there is no qualitative difference between $\delta = -90^\circ$ and $\delta = 90^\circ$ cases. The case with the weak coupling and strong primary and secondary reflections is the same as the case considered here.

5.1.4. Strong secondary and weak primary and coupling reflections. This case is very interesting and its phase sensitivity can be very high. The results of a detailed phase-dependent analysis of this case will be reported elsewhere. In particular, Chao *et al.* (2002) have already demonstrated the high phase sensitivity of this case for macromolecular crystals. The case of strong coupling and weak primary and secondary reflections is the same as the case mentioned here.

5.1.5. Strong primary and weak secondary and coupling reflections. The phase sensitivity of this case can also be high. However, in contrast to the previous high-phase-sensitive cases, the visibility of this case is low. It means that the deviation of the three-wave intensity from the two-wave one is rather small. The condition of the low visibility of three-wave diffraction is given as

$$|A_n|, |B_n| \text{ and } |C_n| \ll 1. \qquad (22)$$

5.2. Bragg angles close to 45°

The polarization state of the incident radiation plays an important role in revealing the phase effect on the diffracted intensity for cases with Bragg angles rather close to 45°. Some new variety of combinations of the values of parameters A_n,

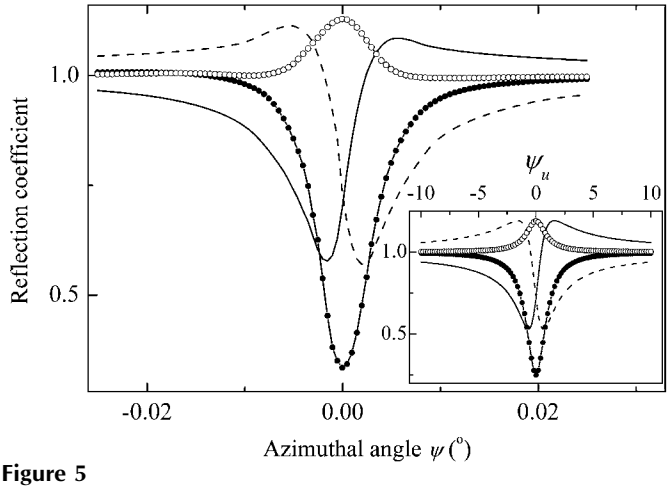

Figure 5
Calculated profiles for GaAs(000, 111, 220) three-wave diffraction for the π-polarized incident radiation with $\lambda = 1.24$ Å. Curves with open circles, solid line, solid circles and dashed line correspond to $\delta = -90$, 0, 90 and 180°, respectively. Inset: profiles calculated according to the iterative approximation with the same conditions.

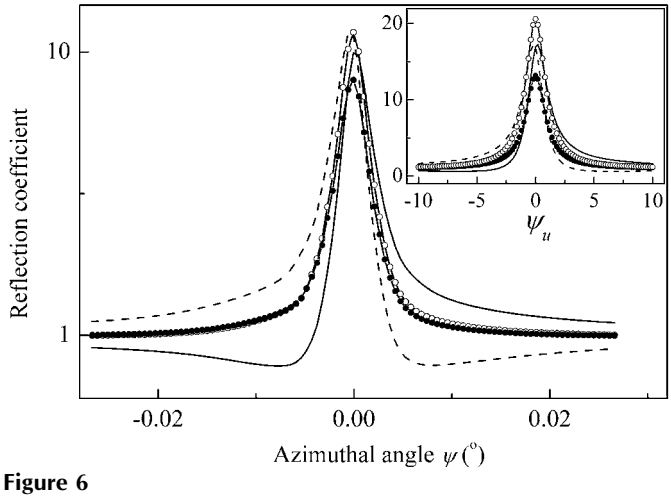

Figure 6
Calculated profiles for GaAs(000, 222, 311) three-wave diffraction for the σ-polarized incident radiation with $\lambda = 1.24$ Å. Curves with open circles, solid line, solid circles and dashed line correspond to $\delta = -90$, 0, 90 and 180°, respectively. Inset: profiles calculated according to the iterative approximation with the same conditions.

B_n and C_n takes place. Under this circumstance, the cases with the different phase sensitivity, high or low, will be considered below. On the one hand, the use of the Bragg angles close to 45° allows the phase sensitivity of three-wave diffraction to be increased by the partial suppression of the stronger *Umweg* wave when the Bragg angles of the secondary or coupling reflection are close to 45° (Stetsko *et al.*, 2000), and by the partial suppression of the stronger primary wave when the Bragg angle of the primary reflection is close to 45° (Kshevetskii *et al.*, 1985; Stetsko *et al.*, 1999; Stetsko, Juretschke *et al.*, 2001; Morelhão & Avanci, 2001; Morelhão & Kycia, 2002; Morelhão, 2003). However, the use of the Bragg angles close to 45° essentially complicates the interpretation of the phase dependence of three-wave diffraction when the primary and *Umweg* waves are equally strong. It should be noted that Morelhão & Kycia (2002) erroneously used the conception of partial suppression of primary reflection (when θ_G is close to 45°) for a comparably weak primary reflection. The case presented in this paper with a high phase sensitivity is attributed to the partial suppression of the *Umweg* wave with the Bragg angle of the secondary reflection being close to 45°.

When the Bragg angles are rather close to 45°, the polarization factors of the primary, *Umweg*- and *Aufhellung*-excited waves [equations (13)–(15)] now have a strong influence upon the change of the values of parameters A_n and B_n with the change of the polarization state (ω) or the wavelength of the incident radiation. Sometimes, the values of parameters A_n and B_n can be dramatically different. This allows the new phase-dependent features of the three-wave diffraction to be detected. It should be noted that, in particular, the essential change of the values of parameters A_n and B_n can be obtained by the use of the π polarization ($\omega = 90°$) with the change of the wavelength of the incident radiation. The experimental approach for investigation of the phase dependence of multiple-wave diffraction with the use of π-polarized X-ray synchrotron radiation of different energies has some technical advantages compared to that with different (intermediate) polarizations ω for a fixed energy.

In §4, we showed that the inversion of peak-profile asymmetry with the change of the polarization state of the incident radiation is accompanied by the change of the sign of the parameter A_n. This inversion is also accompanied by the change of the sign of the parameter B_n. For the inverse case, when the values of parameters A_n and B_n are both negative, the three-wave diffraction exhibits the well known 'inversed' phase-dependent order of peak-profile asymmetry (compared to the σ-polarized incident radiation). The 'inversed' order means that the peak profiles I_G *versus* ψ are still asymmetric for $\delta = 0°$ and $\delta = 180°$, but the intensity first increasing then decreasing for $\delta = 0°$ and first decreasing then increasing for $\delta = 180°$. And the profiles are still practically symmetric for $\delta = -90°$ and $\delta = 90°$, but the intensity for $\delta = -90°$ is now weaker than for $\delta = 90°$.

However, changing of the signs of parameters A_n and B_n may take place under somewhat different conditions of the incident wave, such as different polarizations ω at a fixed wavelength and different wavelengths at fixed polarization. Thus, for a given incident wave, the following cases can be realized: when the value of $|B_n|$ is much less than $|A_n|$ (case of §5.2.1), when the value of $|A_n|$ is much less than $|B_n|$ (case of §5.2.3), and when the signs of parameters A_n and B_n are different (case of §5.2.2). For the later case, the three-wave diffraction exhibits a new 'mixed' phase-dependent order of peak-profile asymmetry. In particular, for a positive A_n and negative B_n, the 'mixed' order means that for $\delta = 0°$ and $\delta = 180°$ the relation between the peak-profile asymmetries is the same as for the 'usual' order while for $\delta = -90°$ and $\delta = 90°$ the relation is the same as for the 'inversed' order.

For cases with Bragg angles close to 45°, the proposed kinematical approach gives the most essential errors compared to the direct dynamical calculations for estimation of the polarization states of diffracted waves. The qualitatively

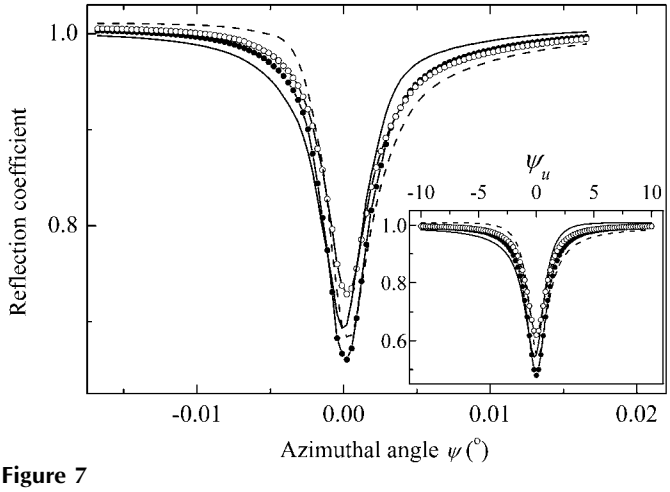

Figure 7
Calculated profiles for GaAs(000, 311, 222) three-wave diffraction for the π-polarized incident radiation with $\lambda = 1.24$ Å. Curves with open circles, solid line, solid circles and dashed line correspond to $\delta = -90$, 0, 90 and 180°, respectively. Inset: profiles calculated according to the iterative approximation with the same conditions.

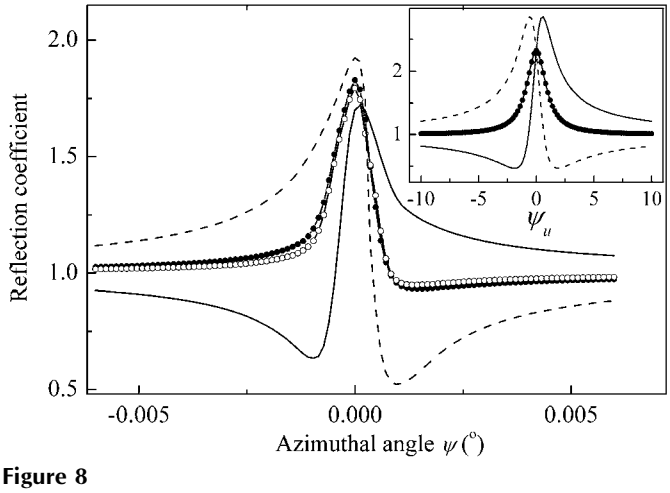

Figure 8
Calculated profiles for Si(000, 331, 313) three-wave diffraction for the π-polarized incident radiation with $\lambda = 1.4$ Å. Curves with open circles, solid line, solid circles and dashed line correspond to $\delta = -90$, 0, 90 and 180°, respectively. Inset: profiles calculated according to the iterative approximation with $\lambda = 1.26$ Å.

similar phase behavior of three-wave diffraction obtained by these two calculation approaches is seen for slightly different polarization states of the incident radiation, *i.e.* of the order of several arc degrees in ω, or around several hundredths of Å for the wavelength of the incident radiation. These differences will be indicated in the figure insets.

The Si(000, 331, 313) three-wave diffraction with strong reflections is investigated in all cases (§§5.2.1–5.2.4, see Figs. 8–12). The π-polarized incident radiations with different wavelengths are considered as the first two cases (§§5.2.1 and 5.2.2). When the wavelength of the incident radiation is so small that the values of all Bragg angles are much less than 45°, the values of parameters A_n and B_n are both positive and the three-wave diffraction exhibits the 'usual' phase-dependent order of peak-profile asymmetry. When the wavelength is increased, the parameter B_n goes to zero for this three-wave diffraction, while the parameter A_n is different from zero.

5.2.1. $|B_n|$ is much less than $|A_n|$. From direct dynamical calculations (Fig. 8), this takes place when the wavelength of the π-polarized incident radiation is around λ = 1.4 Å. The Bragg angles of reflections are $\theta_G = \theta_L = 34.2°$ and $\theta_{G-L} = 21.4°$. The value $|B_n|$ of (20) is much less than $|A_n|$ and A_n = 2.0, $B_n = 0$ and $C_n = 1.33$. Since B_n is the coefficient of sin δ in (20) and close to zero, the diffracted intensity profiles for $\delta = 90°$ and $\delta = -90°$ are almost indistinguishable. This case demonstrates the partially low phase sensitivity for triplet phases close to ±90°. Moreover, when the value of the parameter C_n is also close to zero, *i.e.* when $I_G(\psi_u)/I_2 = 1 + A_n\psi_u \cos\delta/(\psi_u^2 + 1)$, only the peak-profile asymmetry for triplet phases $-90 < \delta < 90°$ is different from that for $90 < \delta < 270°$, while within the region $-90 < \delta < 90°$ (or $90 < \delta < 270°$) the shapes of peak profiles are qualitatively indistinguishable

5.2.2. 'Mixed' phase-dependent order of peak-profile asymmetry (different signs of parameters A_n and B_n). Now the wavelength of the π-polarized incident radiation is changed from 1.4 to 1.48 Å. The Bragg angles of reflections are $\theta_G = \theta_L = 36.4°$ and $\theta_{G-L} = 22.7°$. The value of parameter B_n becomes negative when the value of A_n is still positive, *i.e.* A_n = 2.1, $B_n = -0.4$ and C_n = 2.3. This case demonstrates the above-mentioned 'mixed' phase-dependent order of peak-profile asymmetry as shown in Fig. 9.

The π-polarized incident radiation is often employed for the experimental investigation of the multiple-wave diffraction owing to the better resolution of the monochromated incident beam in the azimuthal direction compared to the σ-polarized radiation. Therefore, the two cases, §5.2.1 and §5.2.2, considered here show how careful the analysis of the phase dependence of multiple-wave diffraction should be when the polarization factors come into play.

The different polarizations ω for the fixed wavelength 1.76 Å of the incident radiation are considered in the final cases, §§5.2.3 and 5.2.4, which demonstrate different phase sensitivity. The Bragg angles of the reflections for the Si(000, 331, 313) diffraction are $\theta_G = \theta_L = 44.9°$ and $\theta_{G-L} = 27.3°$. The three-wave diffractions where two Bragg angles are simultaneously close to 45° are extremely sensitive to polarizations ω of the incident radiation (see the primary and coupling reflections for the case of §4 or the primary and secondary reflections for the present case). When $\omega = 0°$ (σ polarization), the considered three-wave diffraction exhibits the traditional features for diffraction with all strong reflections: a rather high phase sensitivity with positive values of parameters A_n and B_n where the *Aufhellung* component of (7) dominates in this diffraction owing to the negative value of C_n. Similar to the diffraction of §4, with the change of polarization ω in the positive direction, the inversion of the profile asymmetry takes place and the parameters A_n and B_n become negative.

5.2.3. $|A_n|$ is much less than $|B_n|$. From the direct dynamical calculations (Fig. 10), it follows that with the increase of the polarization angle to $\omega = 22°$ the differences between the peak intensities for $\delta = 0°$ and $\delta = 180°$ are negligibly small, while the intensities for $\delta = -90°$ and $\delta = 90°$ are quite different. This

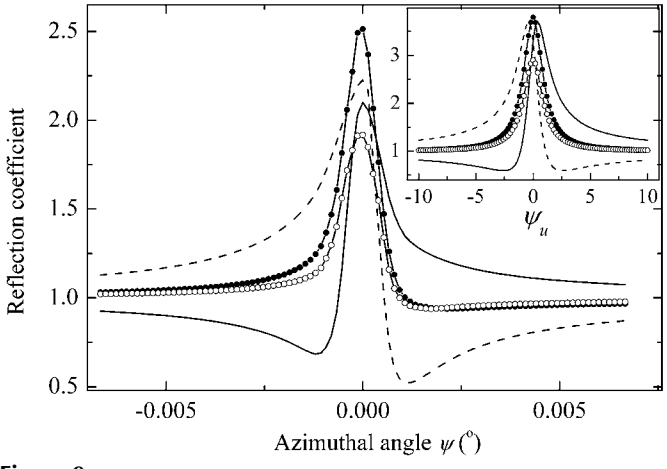

Figure 9
Calculated profiles for Si(000, 331, 313) three-wave diffraction for the π-polarized incident radiation with λ = 1.48 Å. Curves with open circles, solid line, solid circles and dashed line correspond to $\delta = -90$, 0, 90 and 180°, respectively. Inset: profiles calculated according to the iterative approximation with λ = 1.38 Å.

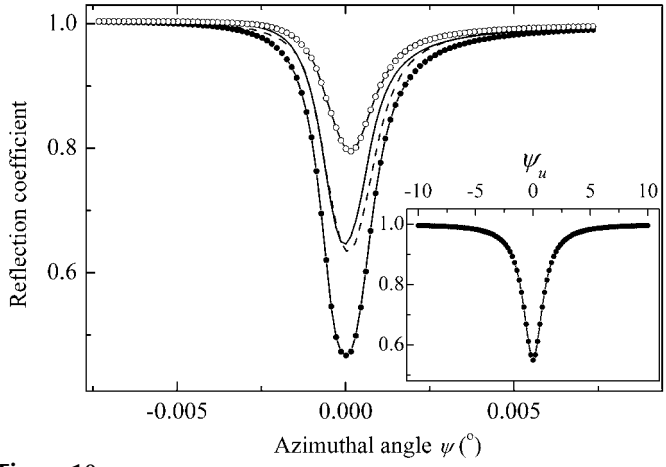

Figure 10
Calculated profiles for Si(000, 331, 313) three-wave diffraction for the polarization $\omega = 22°$ of the incident radiation with λ = 1.76 Å. Curves with open circles, solid line, solid circles and dashed line correspond to $\delta = -90$, 0, 90 and 180°, respectively. Inset: profiles calculated according to the iterative approximation with $\omega = 35.4°$.

situation corresponds to the relation between the parameters of (20) when the value $|A_n|$ is much less than $|B_n|$. Since A_n is the coefficient of $\cos\delta$ in (20) and close to zero, the normalized intensity is $I_G(\psi_u)/I_2 = 1 + (B_n\cos\delta + C_n)/(\psi_u^2 + 1)$. The peak profiles for $\delta = 0^\circ$ and $\delta = 180^\circ$ are practically identical. This case demonstrates the low phase sensitivity; the shapes of peak profiles are qualitatively indistinguishable. However, in contrast to the direct dynamical calculations, the calculations of the proposed kinematical approximation do not show any difference between the intensity profiles for $\delta = -90^\circ$ and $\delta = 90^\circ$ (see inset of Fig. 10 where all curves for different δ coincide). For the considered case when the Bragg angles of the primary and secondary reflections are extremely close to 45°, the value of the parameter B_n is equal to zero simultaneously with A_n. The *Aufhellung* component of (7) still dominates in intensity owing to the negative value of C_n, *i.e.* $C_n = -0.45$.

5.2.4. Parameter C_n close to zero. Because the primary reflection of our diffraction is strong and the Bragg angle is rather close to 45°, the change of the polarization from $\omega = 0$ to $\omega = \pm 90^\circ$ in positive ($0 < \omega < 90^\circ$) or in negative ($-90 < \omega < 0^\circ$) directions leads to the suppression (or partial suppression) of the primary reflection, so that the value of the parameter C_n will change from negative to positive, *i.e.* the *Umweg* component of (7) will overweigh the *Aufhellung* component. Thus, in the positive ($0 < \omega < 90^\circ$) and negative ($-90 < \omega < 0^\circ$) polarization regions, the polarization ω conditions can be realized when the value of the parameter C_n is very close to zero [see also the investigations of Stetsko, Juretschke *et al.* (2001) with a crystal analyzer].

From the direct dynamical calculations, this takes place when the polarization ω is around -30° for the negative polarization region (Fig. 11) and is around 55° for the positive polarization region (Fig. 12). The value of parameters A_n and B_n are both positive for $\omega = -30^\circ$ ($A_n = 1.2$, $B_n = 0.65$ and $C_n = 0$) and negative for $\omega = 55^\circ$ ($A_n = -1.1$, $B_n = -0.81$ and $C_n = 0$). Since C_n is close to zero for both Figs. 11 and 12, the contribution of the phase-independent part to the profile is null and the *Umweg* and *Aufhellung* components of (7) compensate each other. Thus, the intensity profiles are solely phase dependent. The three-wave diffraction exhibits the 'usual' phase-dependent order of peak-profile asymmetry for $\omega = -30^\circ$ and the 'inversed' order for $\omega = 55^\circ$.

Thus, summarizing all the considered cases in §5, the condition of the high phase sensitivity within the framework of the second-order iterative Born approximation is given by

$$|A_n| \sim |B_n|,\ |C_n/A_n| < 1 \text{ and } |C_n/B_n| < 1 \qquad (23)$$

(see also Weckert *et al.*, 1993; Weckert & Hümmer, 1997; and Stetsko *et al.*, 2000; Stetsko, Juretschke *et al.*, 2001 within the framework of the first-order iterative Born approximation).

In conclusion, the second-order iterative Born approximation is adopted for three-wave X-ray diffraction that exhibits the dynamical interaction of the *Umweg* and *Aufhellung* processes. Dependence of the three-wave diffraction profiles of the diffracted wave on the polarization state of a linearly polarized incident wave is theoretically and experimentally investigated. Different cases with low, partially low and high phase sensitivity are theoretically demonstrated. General conditions of the phase sensitivity as well as the visibility and asymmetry of diffraction profiles are obtained within the framework of the second-order iterative approximation and compared with direct dynamical calculations. Reasonable qualitative agreement between the results obtained from this approach and the direct dynamical calculation is shown. A new feature of the 'mixed' phase-dependent order of three-wave peak-profile asymmetries is theoretically predicted. The qualitative increase of the phase sensitivity of multiple-wave diffraction by the partial suppression of the strong primary reflection with the use of the change of the polarization state of a linearly polarized radiation is also demonstrated.

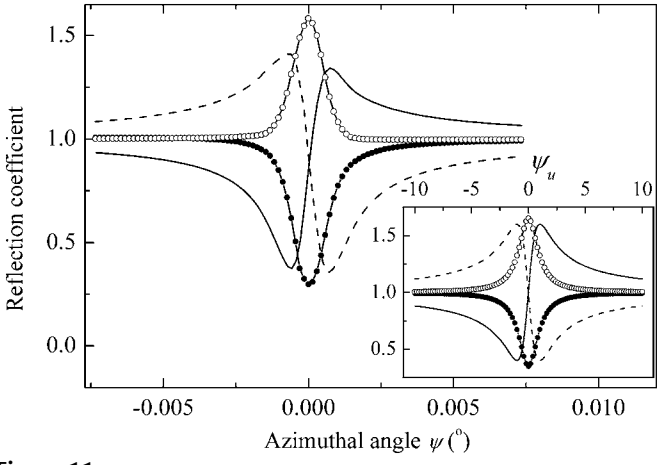

Figure 11
Calculated profiles for Si(000, 331, 313) three-wave diffraction for the polarization $\omega = -30^\circ$ of the incident radiation with $\lambda = 1.76$ Å. Curves with open circles, solid line, solid circles and dashed line correspond to $\delta = -90$, 0, 90 and 180°, respectively. Inset: profiles calculated according to the iterative approximation with $\omega = -33^\circ$.

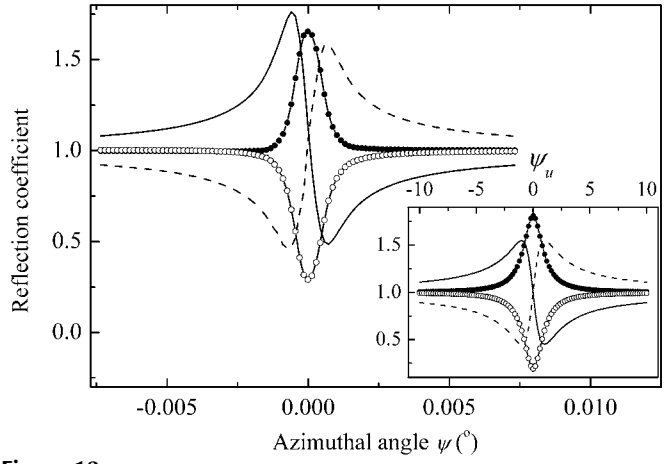

Figure 12
Calculated profiles for Si(000, 331, 313) three-wave diffraction for the polarization $\omega = 55^\circ$ of the incident radiation with $\lambda = 1.76$ Å. Curves with open circles, solid line, solid circles and dashed line correspond to $\delta = -90$, 0, 90 and 180°, respectively. Inset: profiles calculated according to the iterative approximation with $\omega = 61^\circ$.

The authors are indebted to the National Science Council and the Ministry of Education for financial support under contracts No. NSC91-2112-M-213–006 and No. 90-FA04-AA.

References

Caticha-Ellis, S. (1969). *Acta Cryst.* A**25**, 666–673.
Chang, S.-L. (1984). *Multiple Diffraction of X-rays in Crystals.* Heidelberg: Springer-Verlag.
Chang, S.-L. (1987). *Crystallogr. Rev.* **1**, 87–189.
Chang, S.-L. (1992). *Int. J. Mod. Phys.* B**6**, 2987–3020.
Chang, S.-L. (1998). *Acta Cryst.* A**54**, 886–894.
Chang, S.-L., Chao, C.-H., Huang, Y.-S., Jean, Y.-C., Sheu, H.-S., Liang, F.-J., Chien, H.-C., Chen, C.-K. & Yuan, H.-S. (1999). *Acta Cryst.* A**55**, 933–938.
Chang, S.-L., Huang, M.-T., Tang, M.-T. & Lee, C.-H. (1989). *Acta Cryst.* A**45**, 870–878.
Chang, S.-L., Stetsko, Yu. P. & Lee, E.-R. (2002). *Z. Kristallogr.* **217**, 662–667.
Chang, S.-L. & Tang, M.-T. (1988). *Acta Cryst.* A**44**, 1065–1072.
Chao, C.-H., Hung, C.-Y., Huang, Y.-S., Ching, C.-H., Lee, Y.-R., Jean, Y.-C., Lai, S.-C., Stetsko, Yu. P., Yuan, H. & Chang, S.-L. (2002). *Acta Cryst.* A**58**, 33–41.
Colella, R. (1995). *Commun. Condens. Matter Phys.* **17**, 175–215.
Gau, T.-S., Jean, Y.-C., Liu, K.-Y., Chung, C.-H., Chen, C.-K., Lai, S.-C., Shu, C.-H., Huang, Y.-S., Chao, C.-H., Lee, Y.-R., Chen, C.-T. & Chang, S.-L. (2001). *Nucl. Instrum. Methods*, A**466**, 569–575.
Høier, R. & Marthinsen, K. (1983). *Acta Cryst.* A**39**, 854–860.
Hümmer, K. & Billy, H. W. (1986). *Acta Cryst.* A**42** 127–133.
Juretschke, H. J. (1982*a*). *Phys. Rev. Lett.* **48**, 1487–1489.
Juretschke, H. J. (1982*b*). *Phys. Lett.* **92A**, 183–185.
Juretschke, H. J. (1986). *Phys. Status Solidi B*, **135**, 455–466.
Kshevetskii, S. A., Stetsko, Yu. P. & Shelud'ko, S. A. (1985). *Sov. Phys. Crystallogr.* **30**, 270–272.
Larsen, H. B. & Thorkildsen, G. (1998). *Acta Cryst.* A**54**, 129–136.
Luh, S.-W. & Chang, S.-L. (1991). *Acta Cryst.* A**47**, 502–510.
Morelhão, S. L. (2003). *Acta Cryst.* A**59**, 470–480.
Morelhão, S. L. & Avanci, L. H. (2001). *Acta Cryst.* A**57**, 192–196.
Morelhão, S. L. & Kycia, S. (2002). *Phys. Rev. Lett.* **89**, 015501-1–015501-4.
Pinsker, Z. G. (1977). *Dynamical Scattering of X-rays in Crystals.* Berlin: Springer-Verlag.
Shen, Q. (1986). *Acta Cryst.* A**42,** 525–533.
Shen, Q. (1998). *Phys. Rev. Lett.* **80**, 3268–3271.
Shen, Q. (1993). *Acta Cryst.* A**49,** 605–613.
Shen, Q. (1999). *Phys. Rev. Lett.* **83**, 4784–4787.
Shen, Q. (2000). *Phys. Rev. B*, **61**, 8593–8597.
Shen, Q. & Finkelstein, K. D. (1990). *Phys. Rev. Lett.* **65**, 3337–3340.
Shen, Q. & Finkelstein, K. D. (1992). *Phys. Rev. B*, **45**, 5075–5078.
Shen, Q. & Huang, X.-R. (2001). *Phys. Rev. B*, **63**, 174102.
Shen, Q., Kycia, S. & Dobrianov, I. (2000). *Acta Cryst.* A**56,** 268–279.
Stetsko, Yu. P. & Chang, S.-L. (1997). *Acta Cryst.* A**53**, 28–34.
Stetsko, Yu. P. & Chang, S.-L. (1999*a*). *Acta Cryst.* A**55**, 457–465.
Stetsko, Yu. P. & Chang, S.-L. (1999*b*). *Acta Cryst.* A**55**, 683–694.
Stetsko, Yu. P., Chang, S.-L. & Huang, Y.-S. (1999). *Acta Cryst.* A**55** Supplement, Abstract P13.14.015.
Stetsko, Yu. P., Juretschke, H. J., Huang, Y.-S., Chao, C.-H., Chen, C.-K. & Chang, S.-L. (2000). *Acta Cryst.* A**56**, 394–400.
Stetsko, Yu. P., Juretschke, H. J., Huang, Y.-S., Lee, Y.-R., Lin, T.-C. & Chang, S.-L. (2001). *Acta Cryst.* A**57**, 359–367.
Stetsko, Yu. P., Lin, G.-Y., Huang, Y.-S., Chao, C.-H., Chen, C.-K. & Chang, S.-L. (2001). *Phys. Rev. Lett.* **86**, 2026–2029.
Thorkildsen, G. (1987). *Acta Cryst.* A**43**, 361–369.
Thorkildsen, G. & Larsen, H. (2002). *Acta Cryst.* A**58**, 252–258.
Thorkildsen, G., Larsen, H. & Weckert, E. (2001). *Acta Cryst.* A**57**, 389–394.
Wagner, E. (1923). *Phyz. Z.* **21**, 94–98.
Wang, C.-M., Chao, C.-H. & Chang, S.-L. (2001). *Acta Cryst.* A**57**, 420–428.
Weckert, E. & Hümmer, K. (1997). *Acta Cryst.* A**53**, 108–143.
Weckert, E., Schwegle, W. & Hümmer, K. (1993). *Proc. R. Soc. London Ser. A*, **442**, 33–46.
Zachariasen, W. H. (1965). *Acta Cryst.* **18**, 705–710.